JATIS Journal of Astronomical Telescopes, Instruments, and Systems

RESEARCH PAPER

Recovering the dust mass budget with PRIMA

Alberto Traina,[a,*] Francesca Pozzi,[a,b] Francesco Calura,[a] Michele Costa,[a,b] Laura Bisigello,[c] Carlotta Gruppioni,[a] Luigi Barchiesi,[d,e,f] Ivan Delvecchio,[a] Livia Vallini,[a] Cristian Vignali,[a,b] and Viviana Casasola[a,f]

[a]INAF – Osservatorio di Astrofisica e Scienza dello Spazio di Bologna, Bologna, Italy
[b]Università of Bologna, Dipartimento di Fisica e Astronomia, Bologna, Italy
[c]Università of Padova, Dipartimento di Fisica e Astronomia, Padova, Italy
[d]University of Cape Town, Department of Astronomy, Cape Town, South Africa
[e]University of Cape Town, Inter-University Institute for Data Intensive Astronomy, Department of Astronomy, Cape Town, South Africa
[f]INAF-Istituto di Radioastronomia, Bologna, Italy

ABSTRACT. Achieving a complete picture of galaxy evolution is a primary goal of extragalactic astrophysics. To accomplish this ambitious task, a wealth of multiwavelength surveys have been devoted to assessing the cosmic evolution of the cold gas and of the stellar mass across cosmic time. In this cosmic census, one elusive component is represented by interstellar dust. In this work, we exploit the infrared mission PRobe far-Infrared Mission for Astrophysics (PRIMA) (covering wavelengths from 24 to 235 μm) to perform a deep survey (1000 h on 1 deg^2) aimed at estimating the still poorly known dust mass function (DMF) at $z \sim 0.5 - 5$. We consider the spectrophotometric realization of the SPRITZ simulation, and we compute the dust masses using single-temperature modified gray body functions. We show how PRIMA alone, thanks to its unprecedented sensitivities, will constrain the DMF at $z < 1.5$, in terms of mass and faint-end slope. At $z > 1.5$, we stress the key synergy with current or future submillimeter facilities, such as the JCMT/SCUBA-2, AtLAST, LMT, and ALMA telescopes, which will allow us to probe the Rayleigh–Jeans regime of PRIMA selected galaxies. Finally, PRIMA, thanks to its large photometric coverage, will be able for the first time to constrain strictly the warm dust properties of a two-component dust model.

 [DOI: 10.1117/1.JATIS.11.3.031631]

Keywords: ISM: dust; extinction; galaxies: active; galaxies: evolution; galaxies: formation; infrared: galaxies; submillimeter: galaxies; cosmology: early universe

Paper 24242SS received Jan. 2, 2025; revised Apr. 16, 2025; accepted Apr. 17, 2025; published May 14, 2025.

1 Introduction

One major goal of extragalactic astronomy is to trace in the most complete possible way the evolution of baryonic matter across cosmic time. One fundamental component of galaxies is interstellar dust, representing the solid component of the interstellar medium (ISM) and affecting the spectral properties of galaxies over a wide range of wavelengths, ranging from the far-infrared to the ultraviolet domain (e.g., Ref. 1), playing a key role in shaping their evolution.[2–4] How did the dust mass budget evolve through cosmic time? Addressing this question is of the utmost importance to constrain one significant component of the cold mass fraction in galaxies (e.g., Refs. 5–7) to access obscured star formation (e.g., Refs. 8–10) and the fraction of heavy elements removed from the gas phase and incorporated into solid grains (e.g., Refs. 11–14). A fundamental quantity suited for this purpose is the dust mass function (DMF). A thorough

*Address all correspondence to Alberto Traina, alberto.traina@inaf.it

estimate of the evolution of the DMF will allow us to reconstruct how the production and destruction of interstellar dust have changed over time in galaxies of various masses. Thus far, the local DMF has been recovered by various authors (e.g., Refs. 15–17), whereas the evolution of the DMF, based on FIR/sum-mm selection, has been the subject of a handful of studies.[18] considered a sample of 250 μm selected sources from the Herschel-ATLAS Science Definition Phase to look at the evolution of galaxies' space density as a function of their dust mass from $z = 0$ up to redshift $z \sim 0.5$. Their results supported a sharp increase in the bright end of the DMF across this redshift interval, and it has been recently confirmed by Ref. 19 using a sample with an order of magnitude more galaxies than used in previous analyses.

In Ref. 20, the first study of the DMF evolution from $z \sim 0.2$ up to $z \sim 2.5$ has been presented, based on a far-infrared (FIR, 160 μm) Herschel-selected catalog in the COSMOS field. The sample of Ref. 20 consisted of ~5500 sources with flux density > 16 mJy and estimated spectroscopic or photometric redshift. For each of these systems, the dust mass $M_{\rm D}$ was derived from the observed flux by assuming a modified black-body relation, valid for a single-temperature ($T_{\rm D}$) dust component and in the standard optically thin regime.[21,22] This estimate requires the assumption of a temperature value, which comes from an empirical relation among $T_{\rm D}$, star formation rate, and redshift out to $z \sim 2$.[23] However, the observations performed with Herschel suffer from severe limitations due mostly to its poor sensitivity and resolution, which caused significant confusion noise and allowed one to probe only the bright end ($M_{\rm DUST} > 10^9\,{\rm M}_\odot$) of the DMF at $1 < z < 2$. At $z > 3$, there is only one ALMA-based exploration, from Ref. 24. In this work, the authors used ~200 serendipitously detected galaxies from the ALMA AA^{3}COSMOS database[25,26] to sample the DMF at $z = 0.5 - 6$. In the redshift interval in common with Ref. 20 ($0.5 < z < 2.5$), the authors find consistent results but, again, in each redshift bin, they were able to sample only the larger dust masses ($M_{\rm DUST} = 10^9 - 10^{10}\,{\rm M}_\odot$). Thus, a significant component of the DMF (i.e., the faint end, $M_{\rm DUST} \lesssim 10^8\,{\rm M}_\odot$) is currently missing in high-redshift estimates.

Current cosmological simulations allow one to track the evolution of basic galaxy properties, such as star formation, metal content, and dust mass.[27–31] Some current models underpredict the DMF already at $z \sim 1$, fail to account for the characteristic mass, or lack the brightest objects.[32] The present poor theoretical understanding of the evolution of the dust mass budget outlines the need for pursuing more surveys at high redshift to better constrain the shape of the DMF and achieve new estimates at the so-called Cosmic Noon, i.e. at $1 < z < 3$, where the measured peak of cosmic star formation lies. In this paper, we will explore the capabilities of the PRobe far-Infrared Mission for Astrophysics (PRIMA)[33] (PI: GJ. Glenn) to achieve significant progress in the understanding of the dust mass budget evolution as a function of cosmic time. PRIMA is currently in the mission concept phase, with potential approval in 2026. PRIMA is the only instrument that will enable a blind, therefore unbiased IR survey, and thanks to its sensitivity, it will overcome the limitations suffered by Herschel. In this paper, we will show indeed the predictions on the dust mass range and DMF, as probed by PRIMA, using the 60 μm PRIMAger detected sources to the overcome confusion limit at longer wavelengths. With its unprecedented features, PRIMA will

- allow us to improve considerably the characterization of the DMF and the basic parameters that define its shape, enabling a better estimate of the faint end and the sampling of the characteristic dust mass across a wide redshift range;
- extend the redshift range where the dust emission in individual galaxies can be probed, allowing us to derive the DMF, with PRIMA alone data, up to $z = 1.5$ and, in synergy with ALMA, up to $z = 5$;
- allow us to significantly constrain dust production in galaxy formation models, improving our poor theoretical knowledge of this process and filling the gap in our understanding of dust-obscured galaxies.

2 PRIMA Dust Mass Function

2.1 PRIMA

PRIMA is a proposed far-infrared (FIR) observatory, equipped with a 1.8 m diameter mirror and able to perform imaging and spectroscopic studies in the 24 to 235 μm range. PRIMA will be equipped with two instruments: the spectrograph FIRESS and the multiband spectrophotometric

imager PRIMAger. We refer to the PRIMA science book[34] for an exhaustive description of the two instruments, whereas here we remind the main characteristics of PRIMAger, the best instrument among those on board of PRIMA to perform cosmological survey given its high mapping speed, ∼2 dex better than Herschel. PRIMAger consists of two hyperspectral bands with variable filters ($R = 10$, PHI1 and PHI2) in the 24 to 80 μm range and four broad bands filters (PPI1, PPI2, PPI3, and PPI4) in the 80 to 230 μm range. In the following, we will refer only to the total intensity capabilities of PRIMA, and we will consider the two hyperspectral bands PHI1 and PHI2 divided into 12 filters.

2.2 Simulated PRIMA Galaxies and Dust Mass Estimates

To study the improvement achievable on the characterization of DMF, we consider a deep "reference survey" covering 1 deg^2, with a total integration time of 1000 h (overhead included). By this strategy, we achieve 5σ sensitivities in the range 0.09 to 0.23 mJy within the 24 to 230 μm PRIMAger wavelength interval (see the PRIMA fact sheets[35]).

To calculate the expected number of detectable galaxies with PRIMAger, we use the spectro-photometric realizations of IR-selected targets at all z, SPRITZ.[36,37] The SPRITZ simulations are based on a phenomenological model, the starting point of which is the observed IR luminosity function obtained with Herschel data.[38] The SPRITZ model includes different populations of IR active galaxies, such as star-forming galaxies, AGN, and composite systems, along with elliptical galaxies and dwarf irregular galaxies. The SPRITZ simulation produces a catalog of simulated spectral energy distributions (SEDs) (each associated with a specific template), with simulated PRIMA photometry. In our analysis, we used these SEDs to estimate dust masses and temperatures.

Using the SPRITZ realizations, considering the strategy described above, we expect to detect ∼44,000 galaxies with fluxes above the limiting flux of 0.2 mJy in the ninth filter (PHI2 at ∼60 μm). We consider the 60 μm filter as the "detection" filter as it provides the highest observed IR flux, given an IR SED, without reaching the confusion limit (see Ref. 39 for details on the confusion noise) and the benefit of the rapid rise of the IR SED. We plan to use the 60 μm (or lower wavelengths) positions as priors to deblend the longer wavelengths (see Ref. 40). Considering the typical galaxy SEDs of the SPRITZ realizations, we infer a typical 160/60 flux ratio of ∼10 in a large redshift interval ($0.5 < z < 5$, decreasing to ∼3 toward the local universe). This implies a 160 μm detection limit of 2 mJy, nearly 1 dex deeper than Herschel.

We derive $M_{\rm D}$ of the simulated galaxies using a single-temperature modified black body (MBB) in the optically thin approximation (see Ref. 41)

$$M_{\rm D} = \frac{5.03 \times 10^{-31} \cdot S_{\nu_{\rm obs}} \cdot D_{\rm L}^2}{(1+z)^4 \cdot B_{\nu_{\rm obs}}(T_{\rm obs}) \cdot \kappa_{\nu_o}} \cdot \left(\frac{\nu_o}{\nu_{\rm rest}}\right)^{\beta}, \tag{1}$$

where $B_{\nu_{\rm obs}}(T_{\rm obs})$ is the black-body Planck function computed at the observed frame, mass-weighted, temperature ($T_{\rm obs} = T_{\rm D}/(1+z)$); $S_{\nu_{\rm obs}}$ is the flux density at the observed frequency $\nu_{\rm obs}$, with $\nu_{\rm rest} = (1+z)\nu_{\rm obs}$; κ_{ν_o} is the photon cross-section to mass ratio of dust at the rest-frame ν_0; and β is the dust emissivity spectral index. Here, we used $\beta = 1.8$, as suggested value by Ref. 42 based on the findings of Ref. 43 $\kappa = 0.0469$ m^2 kg^{-1}, derived for a wavelength of 850 μm.[44] The dust temperature has been computed for each galaxy following the empirical relation by Ref. 23

$$T_{\rm D} = 98 \times (1+z)^{-0.065} + 6.9 \times \log(SFR/M_{\star}). \tag{2}$$

The applicability of the optically thin approximation is valid in the Rayleigh–Jeans (R-J) regime. This point, along with the possibility of directly deriving the dust temperature $T_{\rm D}$ from the shape of the SED (see also Sec. 3), leads us to adopt two different approaches depending on the galaxy redshift, z: for galaxies at $z < 1.5$, we solely rely on the PRIMAger simulated fluxes, and we use the flux at the longest wavelengths band (230 μm); for galaxies at $z > 1.5$, instead, we extrapolate the expected fluxes at $\lambda > 230$ μm from the simulated SED available in the SPRITZ realizations. This highlights how, at $z \sim 1.5$, the synergy between PRIMA and a sub-millimeter/millimeter telescope such as, for example, JCMT/SCUBA-2, AtLAST, LMT, or ALMA will be fundamental. Indeed, these facilities will allow us to probe the R-J part of the

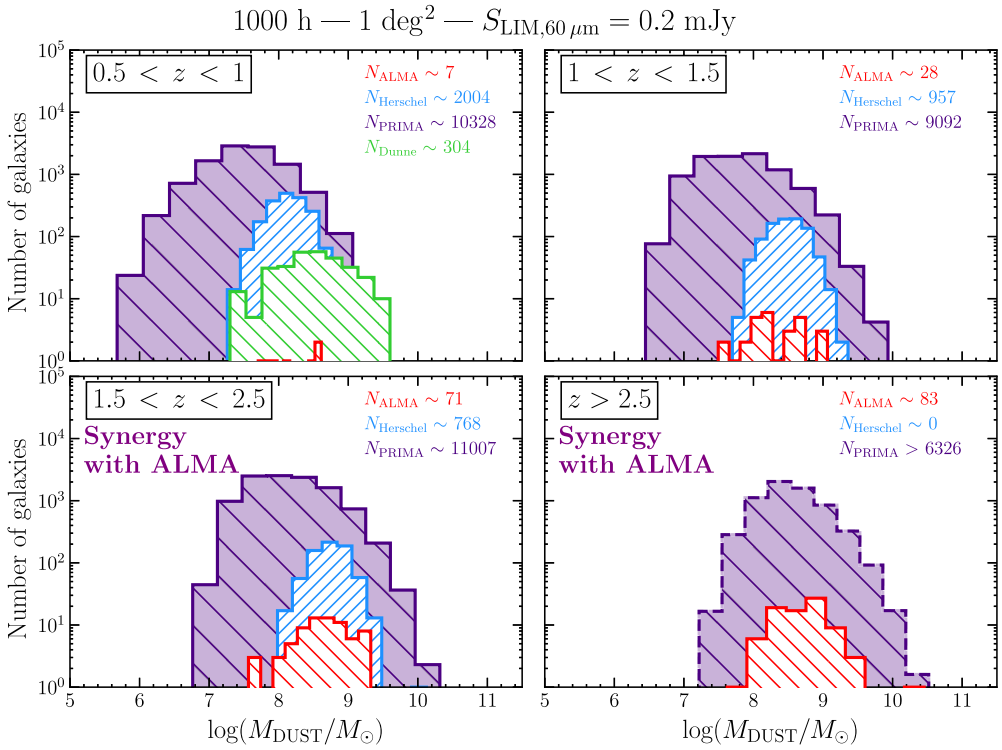

Fig. 1 Dust mass distribution of the galaxies used to derive the DMFs with Herschel (Ref. 20 blue), ALMA (Ref. 24 red), and PRIMA (purple). The distribution of M_{DUST} probed by PRIMA is obtained by leveraging the SPRITZ simulation.[36] As a comparison, the data from Ref. 18 are reported in the top left panel in green.

SED of galaxies selected by PRIMA at shorter wavelength. Given the evergrowing nature of the ALMA archive, we expect the number of PRIMA selected galaxies, with an ALMA counterpart, to reach large statistics in the next ∼10 years (i.e., corresponding to the possible launching date of PRIMA). Other future facilities (e.g., the AtLAST single-dish telescope) will have a fundamental role in probing the R-J part of the SED for a large number of galaxies in relatively short times (e.g., the estimated FoV of AtLAST is expected to be ∼1 deg), reaching limiting fluxes small enough to detect PRIMA-selected galaxies, with an observing time comparable with PRIMA. In Fig. 1, we show the dust mass distribution in four redshift bins that PRIMA will be able to recover with an integration time of 1000 h on 1 deg^2. Together with the PRIMA expectations, the distribution of the dust masses used for the DMF derived with Herschel[20] and ALMA[24] are shown. In all redshift intervals, the number of sources that will be used for the DMF will be at least 1 dex higher than in previous Herschel surveys at $1.5 < z < 5$. Moreover, it is evident how the sensitivities of PRIMA will allow us to extend the mass range of the DMF sampled, especially in the faint end, down to 10^6 M$_\odot$.

2.3 Comparison with Previous DMFs' Estimates

In the past years, several works have been carried out with the goal of deriving the dust properties in the local, as well as in the high-redshift universe, several of which were able to estimate the DMF at $0 < z < 3$.[20,24,45,46] However, except for the lowest redshift bins, even current works are not able to trace the low-mass end of the DMF. This lack of data in the faint end (i.e., $M_{\mathrm{D}} < 10^8$ M$_\odot$) at $z \geq 0.5$ translates into an extrapolation of the Schechter function and into large uncertainties on the population of galaxies with low dust content. Thanks to its photometric coverage and its unprecedented sensitivity, PRIMA is perfectly suited to probe the lowest masses, allowing us to tighten the currently large uncertainties.

In the previous section, we described the method to derive the dust masses, from the observed PRIMA flux densities or by extrapolating each object SED, depending on source redshift. In this section, we discuss the comparison between the predicted PRIMA DMF and those

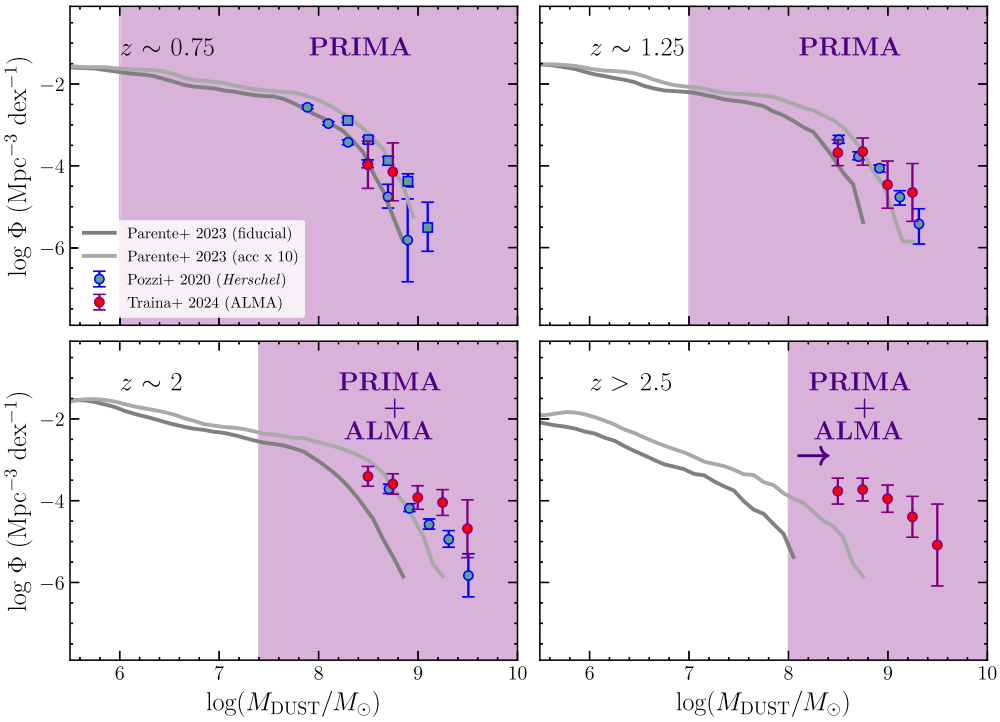

Fig. 2 Dust mass functions at $z \sim 0.75$, $z \sim 1.25$, $z \sim 2$, and $z > 2.5$ from models and literature data, compared with the dust mass range probed by PRIMA. The dark and light gray lines are two different realizations of the SAM by Ref. 47. The first one corresponds to their fiducial model, whereas the second one is derived by reducing the accretion timescale by a factor of 10 to mimic a more efficient accretion in molecular clouds. Data from Refs. 20 and 24 are shown as blue and red points, respectively. Blue squares and circles refer to different redshift bins. The PRIMA predicted DMF is plotted as white diamonds and purple lines.

derived in other works, as well as reducing the uncertainties. Figure 2 shows the comparison between Herschel and ALMA DMFs, with the DMF predicted by PRIMA, in four redshift bins ($0.5 < z < 3$). Even the most recent works have been able to constrain the high-mass end only of the DMF, whereas its knee and faint end remain unprobed. On the other hand, PRIMA will estimate the faint end down to $M_{\mathrm{D}} \sim 10^{6}\,\mathrm{M}_{\odot}$ at $z \sim 0.75$ and $M_{\mathrm{D}} \sim 10^{7}\,\mathrm{M}_{\odot}$ at $0.75 < z < 2$. At very low redshifts (in particular in the first redshift bin), where galaxies with very low dust masses are expected to be detected, we cannot exclude possible effects on the SED shape produced by metallicity. However, the origin of dust in low-metallicity, low-mass galaxies is still largely unknown and has been investigated in only a limited number of studies, even within the local universe,[48–50] making PRIMA even more important in the study of faint sources. At higher redshifts, it is not possible to sample the R-J part of the SED by relying on PRIMA data alone, and ALMA (or other single-dish submillimeter telescopes) data (either proprietary or from the archive) are needed (or extrapolation of the SED at longer wavelengths). The study and characterization of the faint end of the DMF are important not only to extend our knowledge to the faintest galaxies but also to improve the characterization of the physical processes regulating dust formation and evolution in models. In Fig. 2, two sets of semi-analytical models (SAMs) by Ref. 47, with different dust production efficiency, are shown. Even though the characterization of the bright end can help in discriminating among models, however, without a proper sampling of the faint end, it is not possible to fully reconstruct dust properties from models.

The major strengths of PRIMA for the DMF estimate are the wider range covered in wavelength and the larger statistics. From the numbers reported in Fig. 1, we derived the expected improvements in terms of uncertainties in the DMF, compared with the estimates from Herschel and ALMA (see Fig. 3). Assuming that the Poissonian uncertainties on the DMF scale as N^{-2}, where N is the number of objects, PRIMA will improve the error estimates by a factor of 50 to 150 with respect to current ALMA surveys and up to 50 with respect to current Herschel surveys,

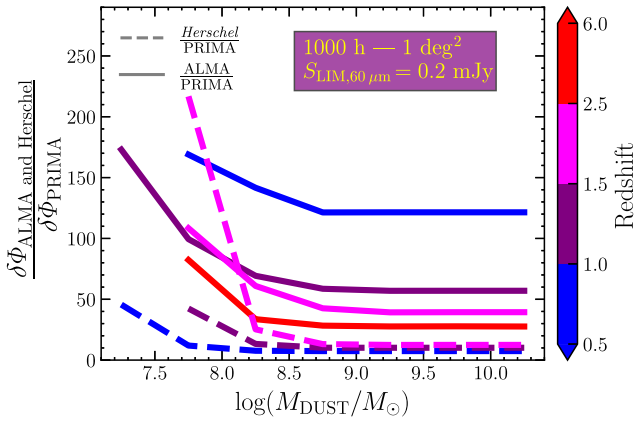

Fig. 3 Ratios between the uncertainties on the DMF as derived by Herschel (dashed line) or ALMA (solid line) and the prediction with PRIMA. Different colors represent different redshift ranges.

up to $z \sim 1.5$. At high redshifts, thanks to the synergy with ALMA, the errors will be improved by a factor of 50 to 100. Figure 3 shows how these uncertainties will be reduced, as a function of the dust mass.

2.4 Synergy with Current and Future (sub-)Millimeter Facilities

As we already mentioned, PRIMA will be able to probe the R-J part of the SED up to $z \sim 1.5 - 2$. At higher redshift, the lack of coverage of the R-J may lead to an inaccurate estimate of the dust masses. For this reason, the synergy of PRIMA with the current of future submillimeter and millimeter facilities (e.g., JCMT/SCUBA-2, LMT, and AtLAST) will be of key importance. In this section, we show how these single-dish telescopes will provide observations on a sky area compatible with the PRIMA 1 deg^2 survey, with lower exposure times (at $z > 2$). From the SPRITZ SED, we derived the flux ratios between the 60 μm and another wavelength at 350 μm $- \lambda - 3$ mm to obtain the sensitivity needed to detect a 60 μm PRIMA detected source at longer wavelengths. From these ratios, using the online ETC for JCMT/SCUBA-2, LMT, and AtLAST, we computed the exposure times required to observe 1 deg reaching the required sensitivity. The results are shown in Fig. 4. At $z > 2$, most of these facilities are able to measure a flux on the R-J and, therefore, will be crucial in the derivation of the dust masses at those redshifts.

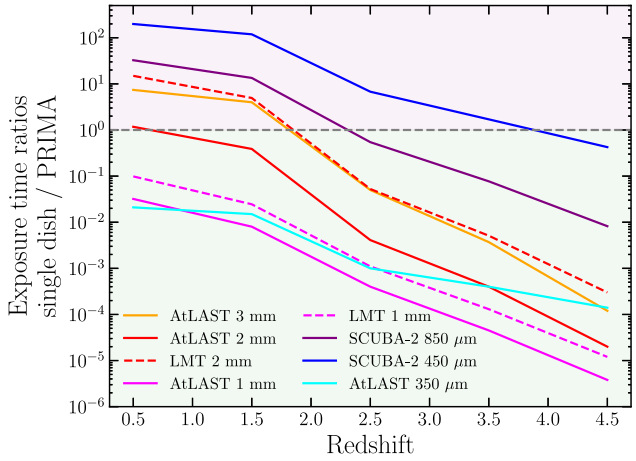

Fig. 4 Ratios between the exposure times of single-dish (sub-)millimeter facilities and PRIMA on 1 deg. Lines with different colors represent different wavelengths, whereas different linestyles are use for different telescopes when plotting curves at the same wavelength. The pink shaded area represents the region in which the exposure times are lower with PRIMA, whereas in the light-green area, single-dish telescopes reach the required sensitivity with lower exposure times.

3 Constraining the Dust Temperature

In Sec. 2.2, we simulate the dust masses by assuming that the FIR emission can be accurately represented by an isothermal MBB function, within the optically thin regime. This simplification provides a good estimate of the bulk of the dust mass, as shown by the comparison between the dust masses derived from the MBB function and those obtained using more complex dust emission models (see Refs. 21 and 22).

In reality, dust grains exhibit a broad range of temperatures, which are determined by both their size distribution and the intensity of the radiation field that heats them.[51] In general, a two-temperature model captures well the diversity in dust temperatures (see Refs. 52 and 53). The two dust components are a warm one (with $20 < T < 60$ K), typically associated with photodissociation regions, and a cold one (with $T < 30$ K) that is primarily linked to the diffuse ISM (see Ref. 54). Figures 5 and 6 show the ability of PRIMAger to constrain the dust masses and temperatures assuming a two-temperature model. In this case, the two components are modeled by two MBB functions. To compute their dust masses from the relation $\tau_\nu = k_\nu \times \Sigma_{\rm dust}$ (with τ_ν being the optical depth), we assumed a power law behavior of the opacity k_ν[55] and a physical size of 10 kpc. The best-fit parameters are retrieved via Markov Chain Monte Carlo fitting implemented with the emcee.[56] In Figs. 5(a) and 5(b), we show the simulated photometry of a main sequence galaxy at $z = 0$ from the SPRITZ realization. Figure 5(a) displays the PRIMAger photometric points, and Fig. 5(b) shows the simulated pre-PRIMA photometric points (Spitzer/MIPS at 24 μm, Herschel/PACS at 65, 96, and 172 μm, and Herschel/*SPIRE* at 250 μm), which represent the current state of the art. The large number of photometric points provided by PRIMAger in the 24 to 230 μm

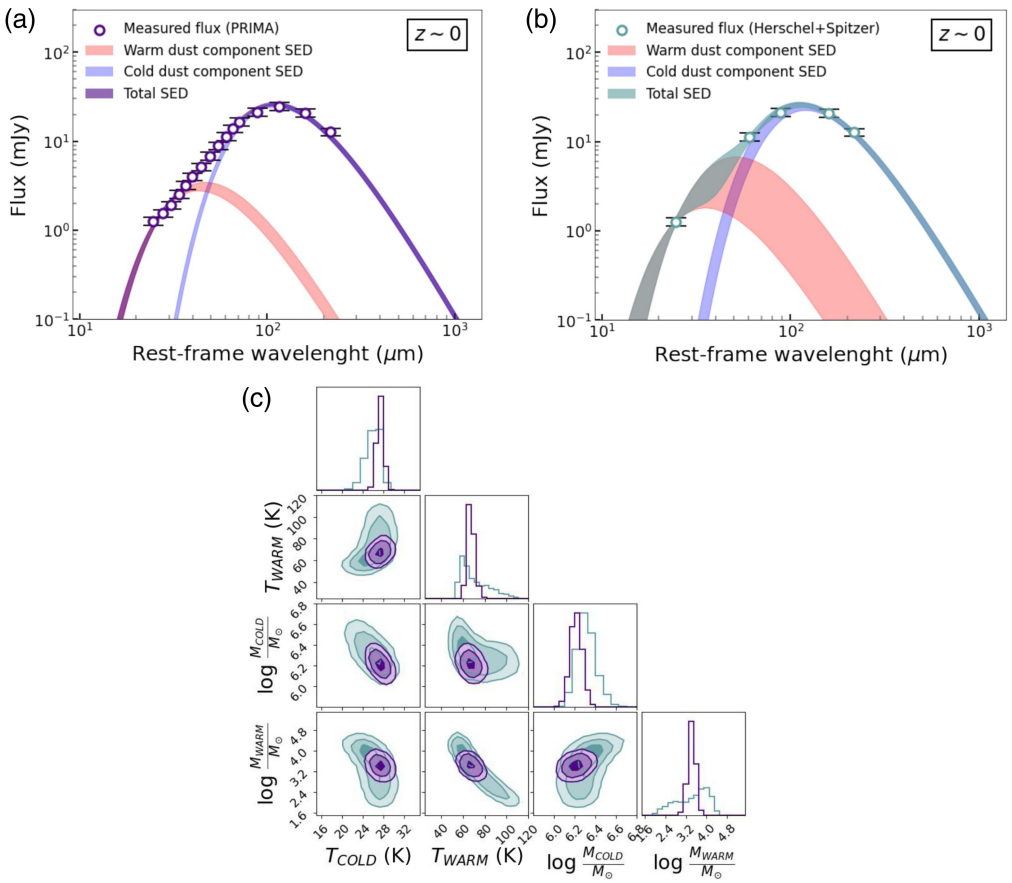

Fig. 5 Simulated photometry of two MS-galaxies at $z = 0$ [(a) and (b)] from the SPRITZ realization.[36] In panels (a) and (b), the pre-PRIMA and PRIMA photometry, respectively, are displayed. The best-fitting two-dust component model is shown in each panel with the associated 1σ uncertainties (red, warm component; blue, cold component). In panel (c), the posterior probabilities of the dust parameters using the pre-PRIMA and PRIMA photometry are shown (blue and violet contours, respectively).

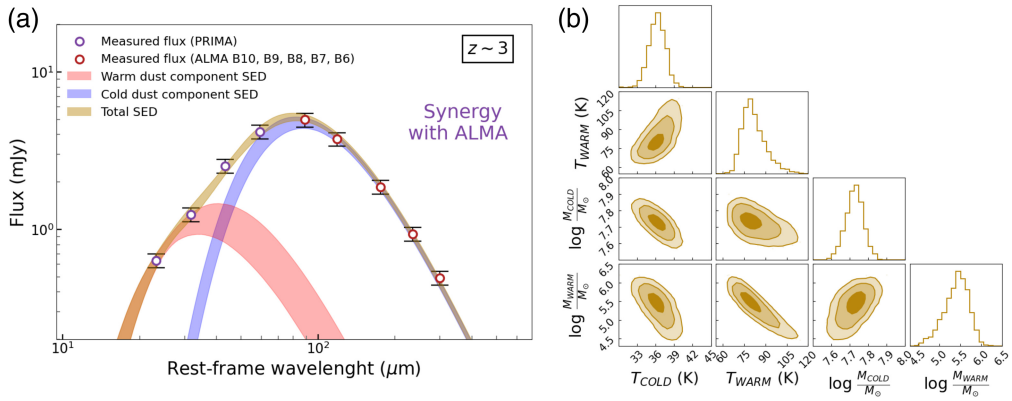

Fig. 6 Simulated PRIMA + ALMA photometry of a galaxy at $z = 3$ (a) from the SPRITZ realization.[36] We display the PRIMA points down to their detection limit (i.e., the other PRIMA bands are below the detection limit).The best-fitting two-dust component model is shown in panel (a) with the associated 1σ uncertainties (red, warm component; blue, cold component). In panel (b), the posterior probabilities of the dust parameters using the PRIMA + ALMA photometry are displayed.

range allows for a very precise determination of the two dust components, at least in the local universe. In particular, considering the warm component, its 1σ mass and temperature ranges are at least a factor of 3 less than those obtained from Spitzer/24 μm + Herschel data [see Fig. 5(c) where the confidence regions are displayed]. In Fig. 6(a), we show the simulated photometry of a galaxy at $z = 3$. Here, the key synergy between PRIMAger and ALMA becomes particularly evident, with PRIMAger effectively constraining the warmer dust component, whereas ALMA is more sensitive to the colder one.

4 Conclusions

In this paper, we explore the performance of the PRIMA instrument PRIMAger, in recovering the DMF as a function of the cosmic time. We have considered a "reference survey" covering 1 deg, with a total integration time of 1000 h. To simulate the galaxies detectable by PRIMAger under this observational strategy, we use the spectrophotometric realization of the SPRITZ code.[36,37] The dust masses have been estimated using a single-temperature MBB model under the optically thin approximation valid in the R-J regime. This led to the adoption of different strategies depending on the redshift z of the sources: for galaxies at $z < 1.5$, we are able to properly constrain the dust emission with just PRIMAger photometry, whereas at $z > 1.5$, we rely on the synergies with the ALMA facility. Our main results are as follows:

- The sensitivities of the PRIMAger instrument, along with the proposed observational survey, will allow us to detect ~44,000 galaxies and derive the DMF across a wide redshift range of $0 < z < 5$. In particular, up to $z \sim 2$, PRIMAger will detect galaxies that are at least 1 dex less massive than those detectable with current facilities. This will allow for better constraints on the faint-end slope of the DMF, which is currently completely unconstrained at $z > 0.5$.
- The large number of galaxies detectable by PRIMAger is able to reduce the uncertainties on the DMF by at least a factor of 50 compared with Herschel-based estimates at $z < 2.5$ and by up to a factor of 50 compared with the high $-z$ DMF measurements obtained with ALMA.
- We have explored the feasibility of fitting the simulated photometry with two dust components (warm and cold). The large number of photometric points provided by PRIMAger will allow to recover of the parameters (mass and temperature) of both components with significantly higher accuracy, with respect to what was possible with previous facilities (e.g., Spitzer and Herschel). We stress how, in particular, the warmer component, traced by the PHI1 and PHI2 filters in the 24 to 80 μm range, will be well constrained for the first time, by reducing its associated uncertainties by at least a factor of 3 in comparison with previous determinations.

Disclosures

The authors declare there are no financial interests, commercial affiliations, or other potential conflicts of interest that have influenced the objectivity of this research or the writing of this paper.

Code and Data Availability

The simulations (from the SPRITZ code)[36] and code developed for the analysis presented in this work are available upon request to the corresponding author. The ancillary data used are from the A^{3}COSMOS database[25] and from the Herschel catalog in the COSMOS field.[20]

Acknowledgments

L.B. acknowledges financial support from the Inter-University Institute for Data Intensive Astronomy, a partnership of the University of Cape Town, the University of Pretoria and the University of the Western Cape, and from the South African Department of Science and Innovation's National Research Foundation under the ISARP RADIOMAP Joint Research Scheme (DSI-NRF Grant No. 150551) and the CPRR HIPPO Project (DSI-NRF Grant No. SRUG22031677). I.D. acknowledges funding by the European Union—NextGenerationEU, RRF M4C2 1.1, Project (Grant No. 2022JZJBHM): "AGN-sCAN: zooming-in on the AGN-galaxy connection since the cosmic noon"—CUP (Grant No. C53D23001120006).

References

1. B. T. Draine, "Interstellar dust models and evolutionary implications," in *Cosmic Dust - Near and Far*, T. Henning, E. Grün, and J. Steinacker, Eds., Astronomical Society of the Pacific Conference Series, Vol. **414**, p. 453 (2009).
2. C. F. McKee and E. C. Ostriker, "Theory of star formation," *Annu. Rev. Astron. Astrophys.* **45**, 565–687 (2007).
3. S. Cazaux and A. G. G. M. Tielens, "Molecular hydrogen formation in the interstellar medium," *Astrophys. J.* **575**, L29–L32 (2002).
4. P. F. Hopkins, E. Quataert, and N. Murray, "Stellar feedback in galaxies and the origin of galaxy-scale winds," *Mon. Not. R. Astron. Soc.* **421**, 3522–3537 (2012).
5. A. Li, "The warm, cold and very cold dusty universe," in *Penetrating Bars Through Masks of Cosmic Dust*, D. L. Block et al., Eds., Astrophysics and Space Science Library, Vol. **319**, p. 535 (2004).
6. P. Santini et al., "The evolution of the dust and gas content in galaxies," *Astron. Astrophys.* **562**, A30 (2014).
7. V. Casasola et al., "Radial distribution of dust, stars, gas, and star-formation rate in DustPedia face-on galaxies," *Astron. Astrophys.* **605**, A18 (2017).
8. A. W. Blain and M. S. Longair, "Observing strategies for blank-field surveys in the submillimetre waveband," *Mon. Not. R. Astron. Soc.* **279**, 847–858 (1996).
9. C. Gruppioni et al., "Tracing the evolution of dust obscured star formation and accretion back to the reionisation epoch with SPICA," *Publ. Astron. Soc. Australia* **34**, e055 (2017).
10. H. S. B. Algera et al., "The ALMA REBELS survey: the dust-obscured cosmic star formation rate density at redshift 7," *Mon. Not. R. Astron. Soc.* **518**, 6142–6157 (2023).
11. F. Calura, A. Pipino, and F. Matteucci, "The cycle of interstellar dust in galaxies of different morphological types," *Astron. Astrophys.* **479**, 669–685 (2008).
12. E. B. Jenkins, "A unified representation of gas-phase element depletions in the interstellar medium," *Astrophys. J.* **700**, 1299–1348 (2009).
13. G. Vladilo et al., "Silicon depletion in damped Lyα systems. The S/Zn method," *Astron. Astrophys.* **530**, A33 (2011).
14. C. Konstantopoulou et al., "Dust depletion of metals from local to distant galaxies. I. Peculiar nucleosynthesis effects and grain growth in the ISM," *Astron. Astrophys.* **666**, A12 (2022).
15. C. Vlahakis, L. Dunne, and S. Eales, "The SCUBA local universe galaxy survey - III. Dust along the Hubble sequence," *Mon. Not. R. Astron. Soc.* **364**, 1253–1285 (2005).
16. D. L. Clements, L. Dunne, and S. Eales, "The submillimetre properties of ultraluminous infrared galaxies," *Mon. Not. R. Astron. Soc.* **403**, 274–286 (2010).
17. R. A. Beeston et al., "GAMA/H-ATLAS: the local dust mass function and cosmic density as a function of galaxy type - a benchmark for models of galaxy evolution," *Mon. Not. R. Astron. Soc.* **479**, 1077–1099 (2018).
18. L. Dunne et al., "Herschel-ATLAS: rapid evolution of dust in galaxies over the last 5 billion years," *Mon. Not. R. Astron. Soc.* **417**, 1510–1533 (2011).

19. R. A. Beeston et al., "Confirming the evolution of the dust mass function in galaxies over the past 5 billion years," *Mon. Not. R. Astron. Soc.* **535**, 3162–3180 (2024).
20. F. Pozzi et al., "The dust mass function from z∼0 to z∼2.5," *Mon. Not. R. Astron. Soc.* **491**, 5073–5082 (2020).
21. S. Bianchi, "Vindicating single-T modified blackbody fits to Herschel SEDs," *Astron. Astrophys.* **552**, A89 (2013).
22. L. K. Hunt et al., "Comprehensive comparison of models for spectral energy distributions from 0.1 μm to 1 mm of nearby star-forming galaxies," *Astron. Astrophys.* **621**, A51 (2019).
23. B. Magnelli et al., "The evolution of the dust temperatures of galaxies in the SFR-M plane up to z2," *Astron. Astrophys.* **561**, A86 (2014).
24. A. Traina et al., "A3COSMOS: dust mass function and dust mass density at $0.5 < z < 6$," *Astron. Astrophys.* **690**, A84 (2024).
25. D. Liu et al., "Automated mining of the ALMA archive in the COSMOS field (A3COSMOS). II. Cold molecular gas evolution out to redshift 6," *Astrophys. J.* **887**, 235 (2019).
26. S. Adscheid et al., "A3COSMOS and A3GOODSS: continuum source catalogues and multi-band number counts," *Astron. Astrophys.* **685**, A1 (2024).
27. M. Parente et al., "Dust evolution with MUPPI in cosmological volumes," *Mon. Not. R. Astron. Soc.* **515**, 2053–2071 (2022).
28. G. Popping, R. S. Somerville, and M. Galametz, "The dust content of galaxies from z = 0 to z = 9," *Mon. Not. R. Astron. Soc.* **471**, 3152–3185 (2017).
29. S. Aoyama et al., "Cosmological simulation with dust formation and destruction," *Mon. Not. R. Astron. Soc.* **478**, 4905–4921 (2018).
30. Q. Li, D. Narayanan, and R. Davé, "The dust-to-gas and dust-to-metal ratio in galaxies from z = 0 to 6," *Mon. Not. R. Astron. Soc.* **490**, 1425–1436 (2019).
31. A. P. Vijayan et al., "Detailed dust modelling in the L-GALAXIES semi-analytic model of galaxy formation," *Mon. Not. R. Astron. Soc.* **489**, 4072–4089 (2019).
32. K.-C. Hou et al., "Dust scaling relations in a cosmological simulation," *Mon. Not. R. Astron. Soc.* **485**, 1727–1744 (2019).
33. https://prima.ipac.caltech.edu/.
34. A. Moullet et al., "PRIMA general observer science book," arXiv:2310.20572 (2023).
35. https://prima.ipac.caltech.edu/page/fact-sheet.
36. L. Bisigello et al., "Simulating the infrared sky with a SPRITZ," *Astron. Astrophys.* **651**, A52 (2021).
37. L. Bisigello et al., "Disentangling the co-evolution of galaxies and supermassive black holes with PRIMA," *Astron. Astrophys.* **689**, A125 (2024).
38. C. Gruppioni et al., "The Herschel PEP/HerMES luminosity function - I. Probing the evolution of PACS selected Galaxies to z 4," *Mon. Not. R. Astron. Soc.* **432**, 23–52 (2013).
39. M. Béthermin et al., "Confusion of extragalactic sources in the far-infrared: a baseline assessment of the performance of PRIMAger in intensity and polarization," *Astron. Astrophys.* **692**, A52 (2024).
40. J. M. S. Donnellan et al., "Overcoming confusion noise with hyperspectral imaging from PRIMAger," *Mon. Not. R. Astron. Soc.* **532**, 1966–1979 (2024).
41. B. Magnelli et al., "The ALMA spectroscopic survey in the HUDF: the cosmic dust and gas mass densities in galaxies up to z3," *Astrophys. J.* **892**, 66 (2020).
42. N. Scoville et al., "The evolution of interstellar medium mass probed by dust emission: ALMA observations at z = 0.3-2," *Astrophys. J.* **783**, 84 (2014).
43. A. Abergel et al., "Planck early results. XXV. Thermal dust in nearby molecular clouds," *Astron. Astrophys.* **536**, A25 (2011).
44. B. T. Draine et al., "Andromeda's dust," *Astrophys. J.* **780**, 172 (2014).
45. L. Dunne, S. A. Eales, and M. G. Edmunds, "A census of metals at high and low redshift and the connection between submillimetre sources and spheroid formation," *Mon. Not. R. Astron. Soc.* **341**, 589–598 (2003).
46. B. Magnelli et al., "The IRAM/GISMO 2 mm survey in the COSMOS field," *Astrophys. J.* **877**, 45 (2019).
47. M. Parente et al., "The $z \lesssim 1$ drop of cosmic dust abundance in a semi-analytic framework," *Mon. Not. R. Astron. Soc.* **521**, 6105–6123 (2023).
48. D. B. Fisher et al., "The rarity of dust in metal-poor galaxies," *Nature* **505**, 186–189 (2014).
49. S. Lianou et al., "Dust properties and star formation of approximately a thousand local galaxies," *Astron. Astrophys.* **631**, A38 (2019).
50. F. Calura et al., "Constraints on the C II luminosity of a proto-globular cluster at z6 obtained with ALMA," *Mon. Not. R. Astron. Soc.* **500**, 3083–3094 (2021).
51. B. T. Draine, "Scattering by interstellar dust grains. I. Optical and ultraviolet," *Astrophys. J.* **598**, 1017–1025 (2003).
52. M. Galametz et al., "Mapping the cold dust temperatures and masses of nearby KINGFISH galaxies with Herschel," *Mon. Not. R. Astron. Soc.* **425**, 763–787 (2012).

53. G. Orellana et al., "Molecular gas, dust, and star formation in galaxies. I. Dust properties and scalings in 1600 nearby galaxies," *Astron. Astrophys.* **602**, A68 (2017).
54. B. T. Draine and A. Li, "Infrared emission from interstellar dust. IV. The silicate-graphite-PAH model in the post-spitzer era," *Mon. Not. R. Astron. Soc.* **657**, 810–837 (2007).
55. S. Carniani et al., "Constraints on high-J CO emission lines in $z \sim 6$ quasars," *Mon. Not. R. Astron. Soc.* **489**, 3939–3952 (2019).
56. D. Foreman-Mackey et al., "emcee: the MCMC hammer," *Publ. Astron. Soc. Pac.* **125**, 306 (2013).

Alberto Traina is a postdoc at the INAF-OAS of Bologna. He received his BS and MS degrees in astrophysics from the University of Bologna in 2018 and 2020, respectively, and his PhD degree in astrophysics from the University of Bologna in 2024. His current research interests include galaxy formation and evolution, as well as their interplay with SMBHs.

Biographies of the other authors are not available.